APPLIED SCIENCE

The International Journal of Applied Sciences.
Vol. 2, No. 1, 2026, pp. 89-114
ISSN 3104-8935

https://international-journal-of-applied-sciences.jo

Effect of Silk Fibroin Peptide Incorporation on the Structural, Mechanical, Thermal, and Biodegradation Properties of Polyurethane

Yusmita Perkasa Damayanti[1a*], **Lilis Abdul Hakim**[2b]

[1] Department of Mechanical Engineering, Faculty of Engineering and Technology, Sampoerna University, Jakarta Selatan 12780, Indonesia, yusmitaperkasa@sampoernauniversity.ac.id

[2] Department of Mechanical Engineering, Faculty of Engineering and Technology, Sampoerna University, Jakarta Selatan 12780, Indonesia, lilisabdul.hakim@sampoernauniversity.ac.id

* Corresponding Author: Yusmita Perkasa Damayanti, yusmitaperkasa@sampoernauniversity.ac.id

DOI: https://doi.org/10.64440/IJAS/IJAS1003

ARTICLE INFO

Article history
Received Feb 04, 2026
Revised Feb 10, 2026
Accepted Apr 22, 2026

Keywords
Silk fibroin;
GAGA peptide;
Polyurethane;
Peptide chain extender ;
Hydrogen bonding;
Mechanical properties;
Thermal stability;
Shape-memory materials;
Hydrolytic degradation;
Enzymatic stability;
Recyclability.

ABSTRACT

Silk fibroin is a naturally occurring protein characterized by a hierarchical molecular structure, abundant repetitive peptide sequences, extensive hydrogen bonding, excellent mechanical strength, and favorable biocompatibility. Inspired by the molecular architecture of silk fibroin, this study investigates the effect of incorporating silk fibroin-derived GAGA (Gly-Ala-Gly-Ala) peptide structures into polyurethane (PU) backbones on their structural, mechanical, thermal, shape-memory, recyclability, and degradation-related properties. A series of peptide-containing diamine chain extenders were synthesized and incorporated into polyurethane based on polycaprolactone diol (PCL2000) and 4,4′-methylenebis(phenyl isocyanate) (MDI). Polyurethanes containing different peptide architectures and peptide contents were prepared and compared with peptide-free polyurethane controls.

Fourier-transform infrared spectroscopy confirmed successful incorporation of peptide structures into the polyurethane backbone. Deconvolution of the carbonyl region demonstrated that peptide incorporation increased the hydrogen-bonded carbonyl fraction from approximately 25% in the control materials to 30.9% in the DC6 polyurethane. The enhanced hydrogen-bonding network produced pronounced improvements in mechanical performance. The tensile strength increased from 29.3 MPa for peptide-free polyurethane to 50.9 MPa for the DC6 material. Peptide incorporation also substantially improved shape-memory performance, with the shape-fixity ratio increasing from 74.3% in the control material to 100% in DC6. Thermal analysis revealed enhanced thermal stability, with the 5% mass-loss temperature increasing from 226.9 to 283.2 °C and the maximum thermal decomposition temperature increasing from 274.1 to 357.6 °C.

The incorporation of peptide structures also modified the degradation behavior of the polyurethane. Peptide-containing materials exhibited increased hydrolytic susceptibility in phosphate-buffered saline and in a lipase-containing aqueous environment at 37 °C, consistent with the greater hydrophilicity introduced by the peptide segments. Nevertheless, the mass loss remained below 3% during the seven-day evaluation period, indicating that the materials retained substantial structural stability under the investigated physiological and enzymatic conditions. Peptide-containing polyurethanes also demonstrated improved retention of mechanical properties after recycling.

Overall, the findings demonstrate that silk fibroin-inspired peptide incorporation provides an effective molecular strategy for regulating the structure–property relationships of polyurethane. The peptide segments function as additional hydrogen-bonding domains that simultaneously enhance mechanical strength, thermal stability, shape-memory behavior, recyclability, and tunable degradation-related characteristics. These findings provide a molecularly informed approach for developing multifunctional polyurethane materials with potential applications in biomedical engineering, smart materials, and advanced recyclable polymer systems.

APPLIED SCIENCE

The International Journal of Applied Sciences.
Vol. 2, No. 1, 2026, pp. 89-114
ISSN 3104-8935

https://international-journal-of-applied-sciences.jo

INTRODUCTION

Polyurethane (PU) is one of the most versatile classes of synthetic polymers and has been extensively investigated for applications requiring a combination of flexibility, strength, elasticity, thermal resistance, and processability. Its properties can be tailored over a wide range through modification of the soft and hard segments, chain extenders, molecular weight, degree of phase separation, and intermolecular interactions. This structural versatility has enabled polyurethane to be employed in coatings, elastomers, adhesives, biomedical materials, sensors, smart materials, and numerous other advanced applications.

Increasing environmental concerns and the growing demand for sustainable polymeric materials have encouraged the development of bio-based and bio-inspired polyurethane systems. Natural materials such as starch, cellulose, and silk provide attractive molecular building blocks because they are renewable and contain well-defined functional groups capable of participating in extensive intermolecular interactions. The incorporation of biological structural motifs into synthetic polymers can provide an opportunity to combine the processability of synthetic materials with selected structural and functional characteristics of natural biomolecules.

Silk is particularly attractive in this context because of its exceptional mechanical performance, structural organization, and biological compatibility. Natural silk consists primarily of fibroin fibers surrounded by a sericin layer. Fibroin forms the principal structural component of silk and is largely responsible for its high tensile strength and toughness. The remarkable properties of silk fibroin originate from its highly organized molecular architecture and repetitive amino-acid sequences.

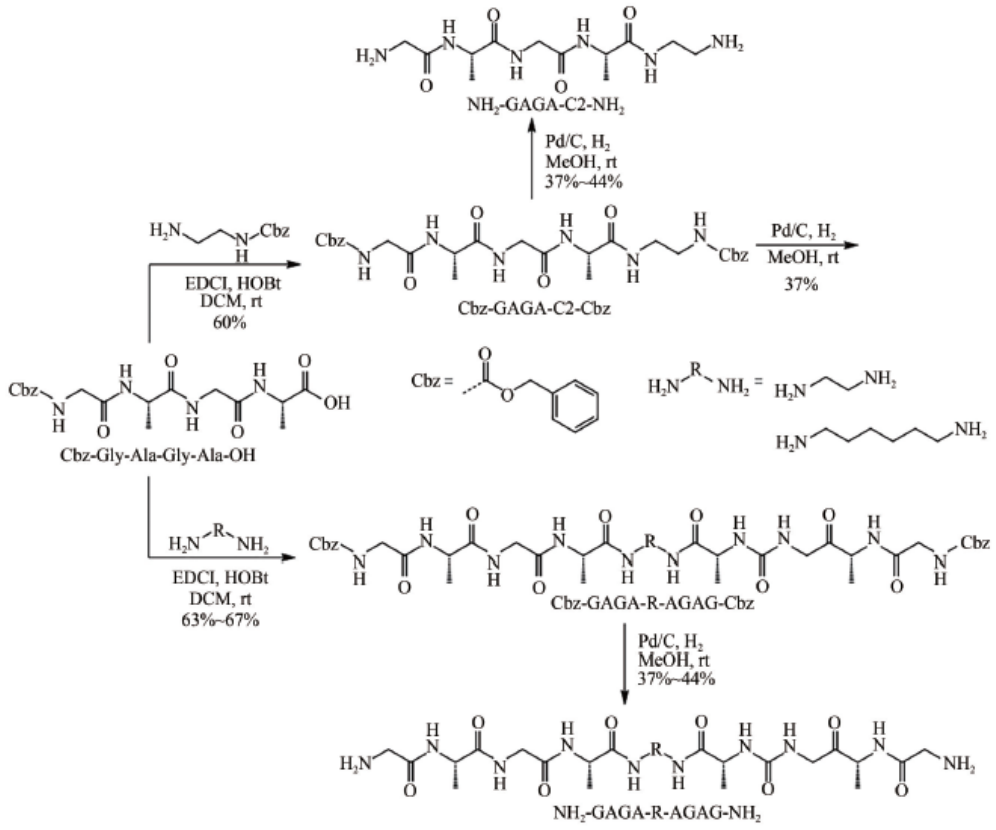

Fig. 1 Synthetic route of tetrapeptide-derived chain extenders.

The International Journal of Applied Sciences.
Vol. 2, No. 1, 2026, pp. 89-114
ISSN 3104-8935
https://international-journal-of-applied-sciences.jo

The heavy chain of silk fibroin contains multiple hydrophobic repetitive domains separated by shorter hydrophilic domains. Among the characteristic repetitive sequences are GAGAGS, GAGAGY, GAGAGA, and GAGYGA motifs. These repetitive peptide structures contribute to the formation of ordered molecular domains and extensive hydrogen-bonding interactions. The resulting molecular organization is an important factor underlying the high mechanical strength, toughness, and structural stability of natural silk.

Natural silk fibroin fibers can exhibit tensile strengths in the range of approximately 300–740 MPa, together with considerable toughness and elongation. The strong intermolecular interactions generated by repetitive peptide segments, particularly hydrogen bonding, play a central role in these properties. Consequently, introducing selected silk fibroin-inspired peptide motifs into synthetic polymers represents a promising strategy for transferring selected structural advantages of natural silk into synthetic polymeric systems.

Previous studies have explored the incorporation of silk fibroin into polyurethane through physical blending, surface coating, electrospinning, and chemical modification. Silk fibroin/polyurethane systems have demonstrated potential in antibacterial materials, wound dressings, sensors, flexible devices, and other biomedical applications. However, most previous approaches have treated silk fibroin as a relatively large molecular component rather than isolating and incorporating its characteristic peptide motifs directly into the polymer backbone.

This distinction is scientifically important. Direct incorporation of structurally defined peptide sequences provides a molecular-level approach for investigating how specific biological motifs influence the properties of synthetic polymers. Rather than relying on the complex structure of the entire silk fibroin protein, peptide-based chain extenders allow the contribution of selected amino-acid sequences to be systematically investigated.

Hydrogen bonding is particularly important in polyurethane because it can regulate chain mobility, intermolecular cohesion, microphase separation, mechanical strength, thermal behavior, and shape-memory performance. Introducing GAGA-based peptide structures into the polyurethane backbone is therefore expected to increase the number of hydrogen-bonding sites and alter the molecular organization of the polymer.

APPLIED SCIENCE

The International Journal of Applied Sciences.
Vol. 2, No. 1, 2026, pp. 89-114
ISSN 3104-8935
https://international-journal-of-applied-sciences.jo

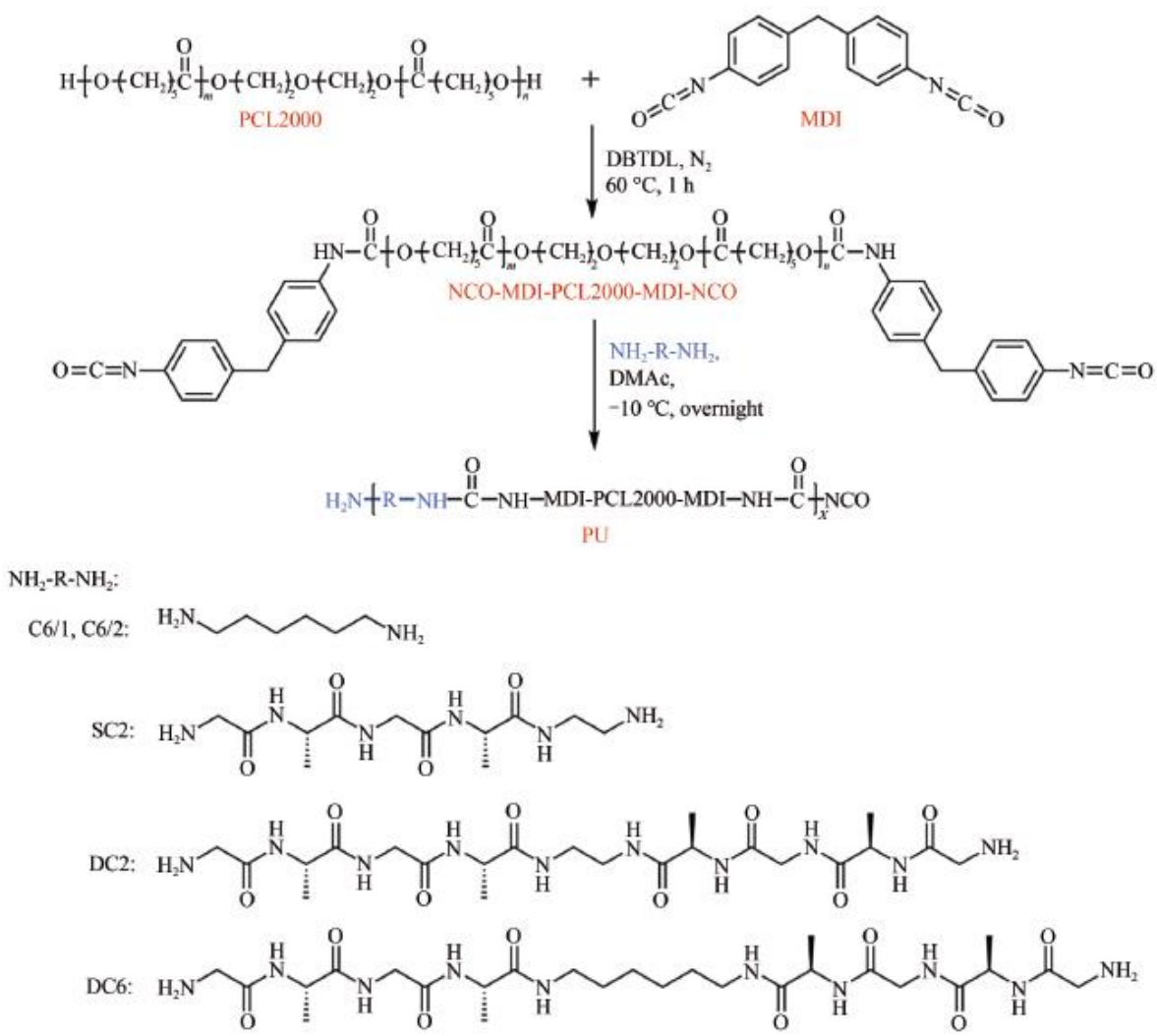

Fig. 2 Synthetic route of polyurethane containing tetrapeptide-derived chain extenders

At the same time, peptide incorporation may influence the interaction of polyurethane with aqueous and biological environments. Peptide segments contain hydrophilic functional groups that can facilitate water penetration into the polymer matrix. Consequently, peptide incorporation may provide an additional means of regulating hydrolytic and enzymatic degradation without necessarily causing rapid loss of structural integrity.

This aspect is particularly relevant to biomedical engineering. Materials designed for biomedical applications often require a carefully controlled balance between mechanical stability, thermal behavior, biological compatibility, water interaction, and degradation resistance. Excessive hydrolysis can result in premature loss of mechanical integrity, whereas excessive stability may limit the suitability of materials for applications requiring controlled degradation.

Shape-memory polyurethane represents another important class of functional materials. Shape-memory behavior depends on reversible changes in polymer-chain mobility and physical interactions. Hydrogen bonds can function as reversible physical crosslinking points, suggesting that peptide incorporation may simultaneously influence mechanical reinforcement and shape-memory behavior.

The International Journal of Applied Sciences.
Vol. 2, No. 1, 2026, pp. 89-114
ISSN 3104-8935
https://international-journal-of-applied-sciences.jo

Despite these opportunities, the relationship between silk fibroin-inspired peptide incorporation, hydrogen bonding, mechanical performance, thermal stability, shape-memory behavior, recyclability, and degradation remains insufficiently understood.

Therefore, the present study develops a molecularly defined peptide-modified polyurethane system using GAGA-derived diamine chain extenders. The study investigates the effect of peptide structure and content on the resulting polyurethane architecture and evaluates the relationships among hydrogen bonding, molecular weight, mechanical properties, thermal stability, shape-memory performance, recyclability, and degradation-related behavior.

The central hypothesis is that incorporation of silk fibroin-inspired GAGA peptide structures into the polyurethane backbone increases intermolecular hydrogen bonding and thereby produces a multifunctional material with enhanced mechanical and thermal properties, improved shape-memory performance, better retention of properties during recycling, and tunable hydrolytic and enzymatic degradation behavior.

2. Materials and Methods

2.1 Materials and Instruments

The principal analytical and mechanical instruments used in this study included a Bruker INVENIO-R Fourier-transform infrared spectrometer (FT-IR), a PL-GPC 120 gel permeation chromatography system, an AGS-X-10 kN universal testing machine, a DSC-Q2000 differential scanning calorimeter, and a Pyris Diamond thermogravimetric/differential thermal analyzer.

Unless otherwise specified, commercially available analytical-grade reagents were used without additional purification.

The principal reagents included N-benzyloxycarbonyl glycine (Cbz-Gly-OH), 1-hydroxybenzotriazole (HOBt), dibutyltin dilaurate (DBTDL), N,N-dimethylformamide (DMF), L-alanine tert-butyl ester hydrochloride, 1-(3-dimethylaminopropyl)-3-ethylcarbodiimide hydrochloride (EDCI), hydrogen chloride/dioxane solution, 1,6-hexanediamine, dichloromethane (DCM), ethyl acetate, methanol, anhydrous N,N-dimethylacetamide (DMAc), palladium on carbon (Pd/C), polycaprolactone diol (PCL2000, Mn ≈ 2000), bromocresol green, anhydrous isopropanol, triethylamine, ethylenediamine, hydrochloric acid, and toluene.

APPLIED SCIENCE

The International Journal of Applied Sciences.
Vol. 2, No. 1, 2026, pp. 89-114
ISSN 3104-8935
https://international-journal-of-applied-sciences.jo

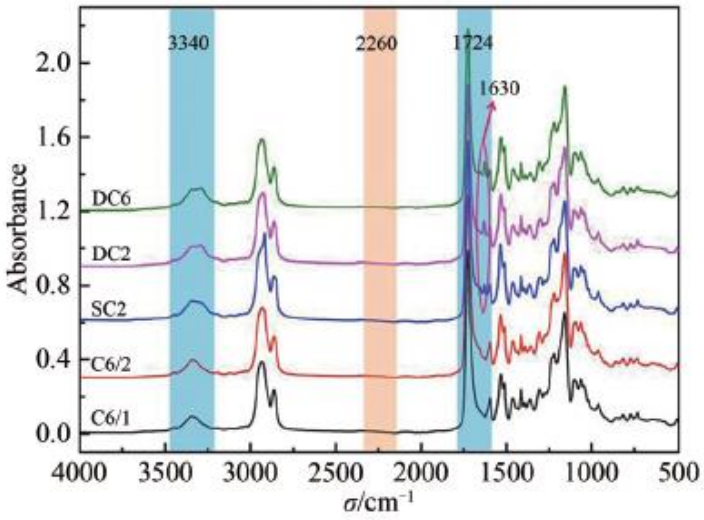

Fig. 3 FT-IR spectra of the polyurethanes

4,4′-Methylenebis(phenyl isocyanate) (MDI) and dibutylamine were also used. Toluene was dehydrated using calcium hydride before use.

2.2 Synthesis of Silk Fibroin-Inspired Peptide Diamine Chain Extenders

2.2.1 Synthesis of the GAGA-Based Tetrapeptide Derivative

The silk fibroin-inspired tetrapeptide derivative N-benzyloxycarbonyl-Gly-Ala-Gly-Ala-OH (Cbz-GAGA-OH) was prepared according to the procedure described in the supporting experimental protocol.

The peptide derivative was subsequently converted into diamine-containing peptide chain extenders suitable for polyurethane synthesis.

2.2.2 Synthesis of NH_2-GAGA-C2-AGAG-NH_2

Cbz-Gly-Ala-Gly-Ala-OH (2.268 g, 5.553 mmol) was dissolved in DCM, followed by the addition of HOBt (0.816 g, 6.039 mmol) and EDCI (1.175 g, 6.129 mmol). The mixture was activated at 0 °C for 30 min. Ethylenediamine (0.148 g, 2.462 mmol) was subsequently added, and the reaction mixture was stirred overnight at room temperature.

After completion, the solvent was removed under reduced pressure. The resulting residue was suspended in acetone, thoroughly mixed, and filtered to obtain the protected peptide intermediate.

The protected intermediate was dissolved in methanol and subjected to catalytic hydrogenation using Pd/C under atmospheric hydrogen for 24 h. Insoluble material was removed by filtration and the solvent was evaporated to obtain the peptide diamine chain extender NH_2-GAGA-C2-AGAG-NH_2.

The isolated yield was 37%.

APPLIED SCIENCE

The International Journal of Applied Sciences.
Vol. 2, No. 1, 2026, pp. 89-114
ISSN 3104-8935
https://international-journal-of-applied-sciences.jo

The molecular structure was characterized by ^{1}H NMR, ^{13}C NMR, and ESI-MS. The experimental mass spectral data were consistent with the expected molecular composition.

2.2.3 Synthesis of NH_2-GAGA-C6-AGAG-NH_2

NH_2-GAGA-C6-AGAG-NH_2 was synthesized using a procedure analogous to that used for NH_2-GAGA-C2-AGAG-NH_2, except that 1,6-hexanediamine was used instead of ethylenediamine.

The isolated yield was 44%. The product was characterized by ^{1}H NMR, ^{13}C NMR, and ESI-MS.

2.2.4 Synthesis of NH_2-GAGA-C2-NH_2

NH_2-GAGA-C2-NH_2 was synthesized using a protected diamine intermediate followed by catalytic hydrogenation. The protected intermediate was dissolved in methanol and hydrogenated in the presence of Pd/C under atmospheric hydrogen for 24 h. After filtration and solvent removal, NH_2-GAGA-C2-NH_2 was obtained with a yield of 37%.

The product was characterized using ^{1}H NMR, ^{13}C NMR, and ESI-MS, confirming formation of the expected peptide-containing diamine structure.

2.3 Preparation of Polyurethane Prepolymer

Polyurethane prepolymer was prepared using PCL2000 as the soft segment and MDI as the hard-segment precursor.

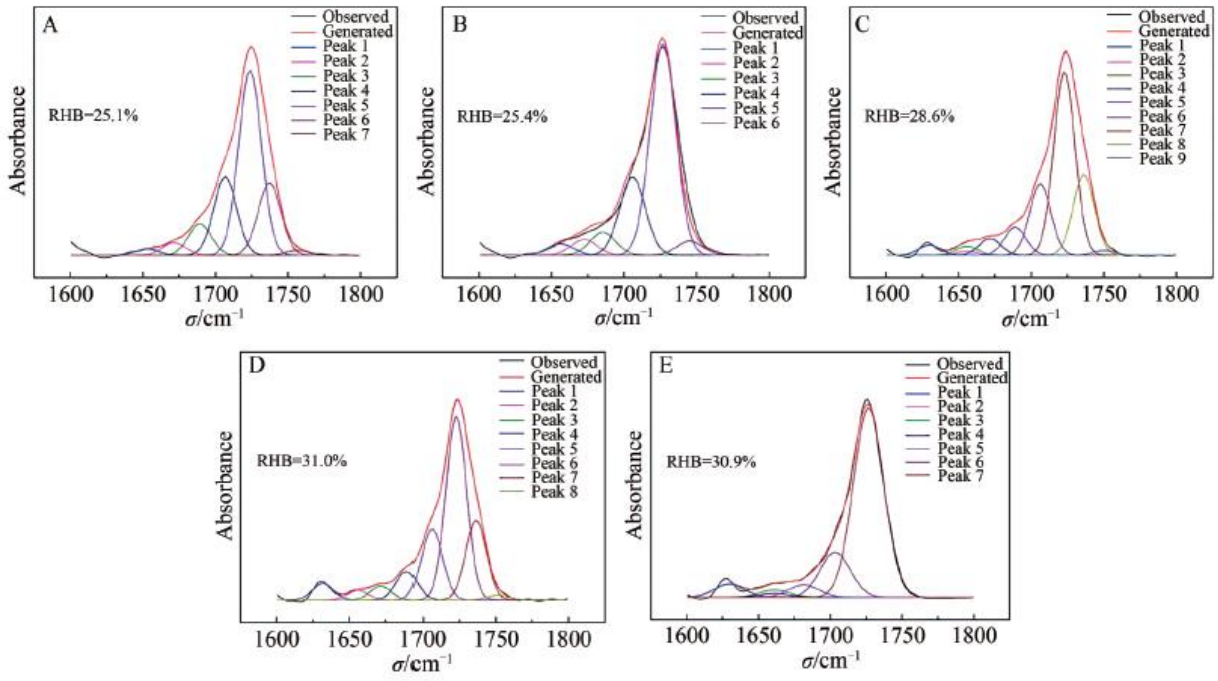

All reaction apparatus was dried under vacuum at 50 °C for 12 h before use.

APPLIED SCIENCE

The International Journal of Applied Sciences.
Vol. 2, No. 1, 2026, pp. 89-114
ISSN 3104-8935
https://international-journal-of-applied-sciences.jo

PCL2000 (1.784 g, 0.892 mmol) was introduced into a three-neck flask and dried under vacuum at 120 °C for 3 h with stirring. Under a nitrogen atmosphere, the flask was cooled to 60 °C, and anhydrous DMAc was added until the PCL2000 was completely dissolved.

In a second three-neck flask, MDI (458 mg, 1.829 mmol) was dissolved in an appropriate quantity of DMAc under nitrogen at 60 °C. The PCL2000 solution was transferred slowly into the MDI solution under reduced pressure using a double-ended needle. The original flask was rinsed three times with DMAc, and the washing solution was transferred to the reaction flask.

The mixture was stirred at 60 °C for 20 min under nitrogen. DBTDL was then added as a catalyst, and the reaction was continued for approximately 40 min to obtain the polyurethane prepolymer.

2.4 Chain Extension and Purification

After completion of prepolymer formation, the reaction mixture was cooled to −10 °C. An aliquot of the prepolymer solution was collected and weighed.

The remaining isocyanate groups were quantified using the toluene–dibutylamine method. The appropriate amount of diamine chain extender was then added according to an NCO_2 molar ratio of 1:1.

The chain-extension reaction was allowed to proceed overnight at −10 °C.

After completion of chain extension, the reaction mixture was precipitated into deionized water to obtain a white solid. The solid was dried and subsequently dissolved in DMF. The solution was reprecipitated, and the resulting solid was dried to obtain purified polyurethane.

For preparation of films, approximately 1 g of polyurethane was dissolved in 15 mL DMF. Insoluble material was removed by filtration, and the filtrate was cast into a polytetrafluoroethylene mold and dried at 50 °C for 48 h.

2.5 Polyurethane Sample Design

Five polyurethane formulations were investigated according to the chain extender employed:

- **C6/1:** 1,6-hexanediamine-based polyurethane with relatively high molecular weight.
- **C6/2:** 1,6-hexanediamine-based polyurethane with relatively lower molecular weight.
- **SC2:** polyurethane containing NH_2-GAGA-C2-NH_2.
- **DC2:** polyurethane containing NH_2-GAGA-C2-AGAG-NH_2.
- **DC6:** polyurethane containing NH_2-GAGA-C6-AGAG-NH_2.

The peptide content was calculated relative to the amount of PCL2000.

The tetrapeptide contents were approximately:

- C6/1: 0
- C6/2: 0
- SC2: 0.52
- DC2: 1.06

APPLIED SCIENCE

The International Journal of Applied Sciences.
Vol. 2, No. 1, 2026, pp. 89-114
ISSN 3104-8935
https://international-journal-of-applied-sciences.jo

- DC6: 1.12

Thus, the experimental design allowed evaluation of both the presence and relative amount of peptide structures as well as the influence of the C2 versus C6 spacer.

3. Characterization and Testing

3.1 Molecular Weight and Molecular-Weight Distribution

Approximately 3 mg of each polyurethane sample was dissolved in 1.0 mL DMF. Gel permeation chromatography was performed at room temperature using DMF as the mobile phase to determine molecular-weight averages and molecular-weight distributions.

The resulting parameters included peak-average molecular weight (Mp), number-average molecular weight (Mn), weight-average molecular weight (Mw), z-average molecular weight (Mz), higher-order molecular-weight averages, viscosity-average molecular weight (Mv), and polydispersity index (PDI).

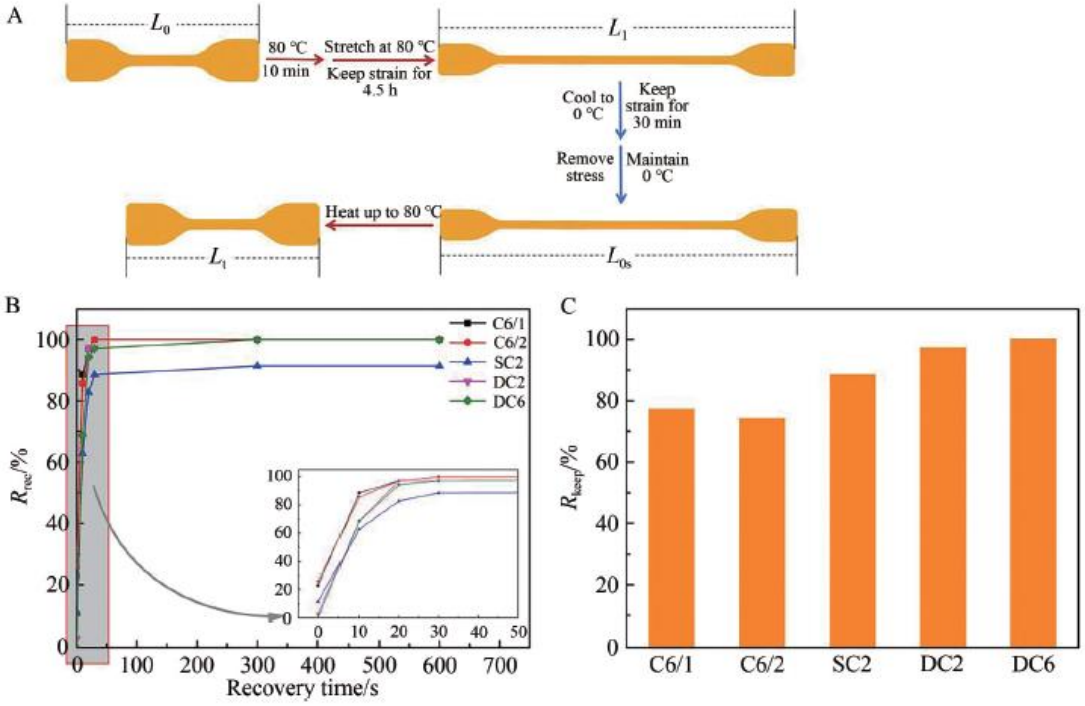

3.2 Fourier-Transform Infrared Spectroscopy

ATR-FTIR spectra were collected using a diamond reflection crystal under an air atmosphere.

Spectra were recorded over the range of 400–4000 cm^{-1} at a resolution of 4 cm^{-1} with 128 scans.

Particular attention was given to the NCO region near 2260 cm^{-1}, the N–H region near 3340 cm^{-1}, the carbonyl region around 1724 cm^{-1}, and the peptide-related amide carbonyl region around 1630 cm^{-1}.

The carbonyl region was deconvoluted to estimate the relative proportion of hydrogen-bonded carbonyl groups.

APPLIED SCIENCE

The International Journal of Applied Sciences.
Vol. 2, No. 1, 2026, pp. 89-114
ISSN 3104-8935

https://international-journal-of-applied-sciences.jo

3.3 Tensile Properties

Polyurethane films were cut into dumbbell-shaped specimens approximately 3.5 cm in total length with a central width of approximately 2.0 mm.

Tensile testing was performed at room temperature using a universal testing machine at a crosshead speed of 50 mm/min.

Tensile strength and elongation at break were recorded.

3.4 Shape-Memory Performance

Dumbbell-shaped polyurethane specimens were thermally activated at 80 °C for 10 min. The specimens were then slowly stretched to a length of 7.0 cm and maintained in the deformed state for 4.5 h.

While maintaining the applied stress, the specimens were transferred to 0 °C for 30 min. The stress was then removed, and the specimens were maintained at 0 °C for an additional 10 min before measuring their length.

The specimens were subsequently returned to 80 °C, and the length change was recorded in real time for up to 600 s.

The shape-recovery ratio was calculated as:

[
R_{rec}=\frac{L_1-L_t}{L_1-L_0}\times100%
]

where L_0 is the initial length, L_1 is the length after deformation at 80 °C, and L_t is the length after t seconds of recovery at 80 °C.

The shape-fixity ratio was calculated as:

[
R_{keep}=\frac{L_{0s}-L_0}{L_1-L_0}\times100%
]

where L_{0s} is the specimen length after relaxation at 0 °C for 10 min.

3.5 Recyclability

Polyurethane films were either cut into small pieces or mechanically stretched to failure and subsequently dissolved in 15 mL DMF.

Insoluble material was removed by filtration. The resulting solution was cast into a PTFE mold and dried at 50 °C for 48 h under atmospheric pressure to produce recycled polyurethane films.

The recycled films were then subjected to tensile testing under the same conditions as the original materials.

The mechanical properties before and after recycling were compared to evaluate the retention of material performance.

The International Journal of Applied Sciences.
Vol. 2, No. 1, 2026, pp. 89-114
ISSN 3104-8935
https://international-journal-of-applied-sciences.jo

3.6 Thermal Properties

Differential scanning calorimetry was performed under nitrogen over the temperature range of −80 to 100 °C using a heating rate of 10 °C/min.

The glass transition temperature (Tg) was determined from the DSC curves.

Thermogravimetric analysis was performed under nitrogen from 25 to 600 °C at a heating rate of 10 °C/min.

The 5% mass-loss temperature (T5%) and maximum decomposition temperature (Tmax) were determined from the thermogravimetric data.

3.7 Hydrolytic and Enzymatic Degradation

To evaluate degradation-related behavior under physiologically relevant conditions, polyurethane films were cut into rectangular specimens measuring approximately 2.0 × 3.0 mm and weighed before incubation.

3.7.1 Hydrolysis in PBS

Specimens were immersed in phosphate-buffered saline (PBS) and incubated at 37 °C.

At days 1, 2, 3, 5, and 7, samples were removed, washed with deionized water, dried, and weighed.

Mass loss was used as an indicator of hydrolytic degradation.

3.7.2 Enzymatic Degradation

A lipase solution with an enzyme activity of approximately 800 U/mL was prepared.

Polyurethane specimens were incubated in the lipase-containing solution at 37 °C.

Samples were collected after 1, 2, 3, 5, and 7 days, washed with deionized water, dried, and weighed.

The degradation behavior was compared with that observed in PBS.

4. Results and Discussion

4.1 Molecular Structure and Successful Peptide Incorporation

The synthesis strategy generated peptide-containing diamine chain extenders incorporating the silk fibroin-inspired GAGA sequence. The resulting chain extenders were subsequently incorporated into the polyurethane backbone through the chain-extension reaction.

The polyurethane system consisted of PCL2000 as the soft segment and MDI as the hard-segment precursor, while either 1,6-hexanediamine or peptide-containing diamines were used as chain extenders.

The peptide-free C6/1 and C6/2 samples contained no GAGA structures. In contrast, SC2, DC2, and DC6 incorporated peptide-derived structures into the main polymer chain.

APPLIED SCIENCE

The International Journal of Applied Sciences.
Vol. 2, No. 1, 2026, pp. 89-114
ISSN 3104-8935
https://international-journal-of-applied-sciences.jo

The peptide contents were 0.52 for SC2, 1.06 for DC2, and 1.12 for DC6. The experimental design therefore provided a systematic basis for investigating the influence of peptide content and molecular architecture.

FTIR analysis provided direct evidence of successful polyurethane formation. No characteristic NCO absorption was observed near 2260 cm^{-1}, indicating substantial consumption of the isocyanate groups during polymerization.

The absorption bands near 3340 cm^{-1} and 1724 cm^{-1} were attributed to N–H and carbonyl groups associated with the polyurethane structure, confirming formation of urethane linkages.

Importantly, SC2, DC2, and DC6 displayed an additional feature near 1630 cm^{-1} that was absent in C6/1 and C6/2. This feature is associated with the carbonyl stretching of amide groups within the peptide structures and therefore provides spectroscopic evidence for incorporation of the GAGA-derived peptide motifs.

These results confirm that the peptide structures were successfully incorporated into the polyurethane backbone rather than simply physically mixed with the polymer.

4.2 Molecular Weight and Hydrogen-Bonding Interactions

The molecular-weight characteristics of the five polyurethane materials are summarized in Table 1.

Table 1. Molecular-weight characteristics of the polyurethane materials

Sample	Mp ×10³	Mn ×10³	Mw ×10³	Mz ×10³	Mz+1 ×10³	Mv ×10³	PDI
C6/1	116	93	426	1736	3344	329	4.57
C6/2	183	68	358	1052	1936	294	5.28
SC2	107	45	179	515	1113	150	4.02
DC2	92	46	226	1007	2418	177	4.86
DC6	130	57	369	1689	3873	282	6.45

The control samples C6/1 and C6/2 displayed substantially different number-average molecular weights, 9.3×10^4 and 6.8×10^4, respectively. However, their hydrogen-bond ratios were nearly identical, at 25.1% and 25.4%.

This observation suggests that the hydrogen-bonding ratio in this polyurethane system is not determined primarily by molecular weight. Instead, the chemical architecture and functional groups present along the polymer backbone appear to be more important.

Incorporation of peptide structures produced a clear increase in the hydrogen-bond ratio. SC2 exhibited an RHB of 28.6%, while DC2 and DC6 exhibited values of 30.0% and 30.9%, respectively.

The progressive increase in RHB with increasing peptide content indicates that the GAGA-derived peptide segments introduce additional hydrogen-bonding sites into the polyurethane matrix.

The highest peptide-containing material, DC6, therefore exhibited approximately 20% more hydrogen-bonded carbonyl groups than the peptide-free controls.

The International Journal of Applied Sciences.
Vol. 2, No. 1, 2026, pp. 89-114
ISSN 3104-8935
https://international-journal-of-applied-sciences.jo

These findings establish an important structure–interaction relationship:

Increasing peptide incorporation → increased hydrogen bonding → stronger intermolecular cohesion.

This molecular interaction is subsequently reflected in the mechanical, thermal, shape-memory, recycling, and degradation-related properties.

4.3 Mechanical Properties

The tensile behavior of the polyurethane materials demonstrated a strong relationship with molecular weight and hydrogen-bonding density.

Among the peptide-free materials, C6/1 exhibited higher tensile strength and rigidity than C6/2, consistent with its higher number-average molecular weight.

SC2 exhibited a lower molecular weight than C6/2 but maintained a comparable tensile strength. Its elongation at break reached 1028%. This behavior indicates that the increased hydrogen-bonding interactions introduced by the peptide structure can compensate for some of the adverse effects associated with reduced molecular weight.

The effect was more pronounced in DC2 and DC6.

DC6 exhibited a tensile strength of 50.9 MPa compared with 29.3 MPa for C6/2. Thus, peptide incorporation increased tensile strength by approximately 74% relative to the C6/2 reference.

This improvement is attributed to the additional hydrogen bonds formed between peptide-containing segments. These interactions behave as reversible physical crosslinking points, increasing resistance to chain slippage and deformation.

The results therefore demonstrate that peptide incorporation provides molecular reinforcement without requiring permanent covalent crosslinking.

This is particularly advantageous for multifunctional polymer systems because reversible interactions can improve strength while preserving the possibility of processing, deformation, shape recovery, and recycling.

4.4 Shape-Memory Performance

The shape-memory properties showed a pronounced dependence on peptide incorporation.

The peptide-free C6/1 and C6/2 materials exhibited shape-fixity ratios below 80%.

SC2, containing a tetrapeptide structure, exhibited a substantially improved shape-fixity ratio approaching 90%.

The bis-tetrapeptide materials DC2 and DC6 exhibited even greater shape-fixity. In particular, DC6 achieved a shape-fixity ratio of 100%, compared with 74.3% for C6/2.

This improvement demonstrates that peptide-derived hydrogen-bonding domains can effectively stabilize the temporarily programmed shape.

APPLIED SCIENCE

The International Journal of Applied Sciences.
Vol. 2, No. 1, 2026, pp. 89-114
ISSN 3104-8935

https://international-journal-of-applied-sciences.jo

During heating at 80 °C, the hydrogen-bond network is partially disrupted and polymer chains become more mobile. After deformation and cooling to 0 °C, chain mobility decreases and hydrogen bonds reform, stabilizing the temporary shape.

Upon reheating, these reversible hydrogen bonds are disrupted again, allowing the polymer chains to regain mobility and return toward the original configuration.

The recovery kinetics were also favorable. Most samples achieved more than 60% recovery within 10 s, while all samples except SC2 exceeded 90% recovery within approximately 20 s. Complete recovery was achieved within approximately 5 min for the investigated materials.

The results demonstrate that peptide incorporation does not simply strengthen polyurethane; it also improves its ability to store and recover mechanically programmed shapes.

4.5 Recyclability

The recycled polyurethane films were successfully regenerated by dissolution in DMF followed by solution casting.

Most recycled materials exhibited some reduction in tensile strength and a corresponding increase in elongation at break. This behavior is likely related to partial molecular-chain damage during mechanical fragmentation and reprocessing.

GPC results also indicated reductions in number-average molecular weight after recycling, confirming that some degree of chain scission or structural damage occurred.

However, the peptide-containing materials retained their mechanical properties more effectively than the peptide-free controls.

C6/1 and C6/2 showed more pronounced decreases in tensile strength after recycling, whereas SC2, DC2, and DC6 exhibited comparatively small changes.

The improved retention is attributed to the reversible hydrogen-bonding interactions generated by the peptide structures.

Unlike permanent covalent crosslinks, hydrogen bonds can dissociate during processing and reform after processing. Consequently, peptide-containing polyurethanes can benefit from reversible physical reinforcement while maintaining reprocessability.

These findings demonstrate an important additional advantage of peptide incorporation: improved resistance to mechanical deterioration during recycling.

4.6 Thermal Stability

Thermogravimetric analysis revealed a substantial improvement in the thermal stability of peptide-containing polyurethane.

The 5% mass-loss temperature increased from 226.9 °C for C6/1 to 283.2 °C for DC6.

This represents an increase of approximately 25%.

The maximum decomposition temperature also increased substantially, from 274.1 °C for C6/1 to 357.6 °C for DC6, corresponding to an increase of approximately 30%.

The improved thermal stability is attributed to the enhanced intermolecular hydrogen-bonding network produced by the peptide segments.

The International Journal of Applied Sciences.
Vol. 2, No. 1, 2026, pp. 89-114
ISSN 3104-8935
https://international-journal-of-applied-sciences.jo

Hydrogen bonds restrict molecular-chain mobility and increase the energy required to disrupt the polymer structure. Consequently, peptide-containing polyurethane requires higher temperatures to initiate substantial thermal degradation.

These findings indicate that GAGA peptide incorporation can improve the thermal robustness of polyurethane and potentially expand its usable temperature range.

4.7 Glass Transition Behavior

The glass transition temperatures of the peptide-free samples were −47.77 °C for C6/1 and −47.97 °C for C6/2.

The similarity between these values further supports the conclusion that molecular weight alone does not strongly control Tg within the investigated range.

In contrast, peptide-containing materials exhibited higher Tg values:

- SC2: −46.61 °C
- DC2: −44.85 °C
- DC6: −46.02 °C

The increase in Tg is consistent with the enhanced hydrogen-bonding interactions introduced by the peptide structures.

The stronger intermolecular interactions restrict segmental motion, requiring additional thermal energy to activate polymer-chain movement.

Therefore:

Peptide incorporation → stronger hydrogen bonding → restricted segmental mobility → increased Tg.

4.8 Hydrolytic Degradation in PBS

The introduction of the degradation-related variable provides additional insight into the interaction between molecular structure and environmental stability.

C6/1 and C6/2 exhibited similar hydrolytic behavior in PBS despite their different molecular weights.

In contrast, peptide-containing materials exhibited increased hydrolytic mass loss.

The extent of hydrolysis increased with peptide content.

This behavior is attributed primarily to the greater hydrophilicity of the peptide-containing chain extenders compared with the hydrophobic 1,6-hexanediamine structure used in the control materials.

The more hydrophilic peptide segments can facilitate water penetration and diffusion into the polymer matrix, increasing access of water molecules to hydrolyzable groups.

However, the increase in degradation remained limited.

The International Journal of Applied Sciences.
Vol. 2, No. 1, 2026, pp. 89-114
ISSN 3104-8935
https://international-journal-of-applied-sciences.jo

All materials exhibited less than 3% mass loss during the seven-day PBS evaluation.

Therefore, peptide incorporation simultaneously increased aqueous accessibility and maintained substantial structural stability.

This balance is important for potential biomedical applications, where excessive hydrolysis can compromise mechanical performance prematurely.

4.9 Enzymatic Degradation Stability

The enzymatic stability of the polyurethane materials was evaluated using a lipase-containing aqueous environment at 37 °C.

The degradation behavior generally followed the trend observed in PBS.

C6/1 and C6/2 exhibited relatively low mass loss, whereas peptide-containing polyurethanes showed increased degradation-related mass loss.

Nevertheless, even in the presence of lipase, all samples remained below 3% mass loss over the seven-day period.

These findings demonstrate that the introduction of peptide structures increases the interaction between polyurethane and the aqueous/enzymatic environment but does not result in rapid material breakdown.

The combination of limited degradation and enhanced mechanical properties indicates that the peptide-containing materials maintain a favorable balance between environmental responsiveness and structural stability.

5. Integrated Structure–Property Relationship

The results collectively reveal a coherent molecular mechanism underlying the multifunctional behavior of the peptide-modified polyurethane.

The incorporation of GAGA-derived peptide structures introduces additional amide groups into the polyurethane backbone.

These groups provide additional hydrogen-bonding sites.

The increased hydrogen-bond density enhances intermolecular cohesion and creates reversible physical crosslinking domains.

These domains then influence several properties simultaneously.

Molecular mechanism

GAGA peptide incorporation

↓

Additional hydrogen-bonding sites

↓

Higher hydrogen-bond ratio

↓

The International Journal of Applied Sciences.
Vol. 2, No. 1, 2026, pp. 89-114
ISSN 3104-8935
https://international-journal-of-applied-sciences.jo

Stronger intermolecular interactions

↓

Restricted chain slippage and segmental motion

↓

Enhanced tensile strength

Enhanced thermal stability

Improved shape-fixity

Improved recycling stability

At the same time:

Peptide incorporation

↓

Greater hydrophilicity

↓

Improved water penetration

↓

Increased hydrolytic/enzymatic susceptibility

while:

Strong hydrogen-bonding network

↓

Preservation of polymer structural integrity

↓

Limited overall degradation

This dual effect represents one of the most important findings of the study.

The peptide structures do not merely reinforce polyurethane. They provide a means of simultaneously controlling mechanical strength, thermal stability, shape-memory behavior, recyclability, and degradation-related behavior through molecular-level modification.

6. Discussion

The present study demonstrates that bio-inspired molecular design can provide a powerful alternative to conventional polymer modification strategies.

The International Journal of Applied Sciences.
Vol. 2, No. 1, 2026, pp. 89-114
ISSN 3104-8935
https://international-journal-of-applied-sciences.jo

Traditional reinforcement approaches often rely on inorganic fillers, nanoparticles, covalent crosslinking, or blending with secondary polymers. Although these approaches can improve individual properties, they may also reduce flexibility, processability, recyclability, or molecular-level control.

The present approach is fundamentally different because it incorporates a structurally defined biological motif directly into the polyurethane backbone.

The GAGA sequence was selected because repetitive glycine- and alanine-rich motifs constitute characteristic structural features of silk fibroin. By incorporating these motifs through diamine chain extenders, the study transfers selected molecular characteristics of silk fibroin into a synthetic polyurethane architecture.

The resulting hydrogen-bonding interactions provide reversible physical reinforcement.

This mechanism explains why DC6 can exhibit substantially greater tensile strength than C6/2 despite having a lower number-average molecular weight.

The results therefore challenge the assumption that molecular weight alone determines the mechanical properties of polyurethane.

Instead, the data indicate that molecular architecture and intermolecular interaction density can compensate for differences in molecular weight.

The same molecular mechanism also explains the improvements in shape-memory behavior.

The reversible hydrogen-bond network acts as a dynamic physical crosslinking system. At low temperature, the hydrogen bonds stabilize the programmed shape, whereas heating disrupts these interactions and increases chain mobility.

This provides a molecular explanation for the 100% shape-fixity observed in DC6.

The thermal results further support this interpretation. Increased hydrogen bonding increases the energy required for chain motion and thermal disruption, resulting in higher Tg and higher thermal decomposition temperatures.

The recycling results are also significant.

Because hydrogen bonds are reversible, they can provide mechanical reinforcement without permanently locking the polymer network. This allows the material to retain relatively favorable mechanical properties after dissolution and reprocessing.

The degradation experiments provide an additional dimension to the structure–property relationship.

The peptide segments increase hydrophilicity and therefore promote greater water interaction. This produces increased hydrolytic susceptibility in PBS and in the lipase-containing environment.

However, the degradation remains limited to less than 3% during the seven-day period.

Therefore, peptide incorporation does not produce uncontrolled degradation. Instead, it appears to shift the equilibrium between water accessibility and structural stability.

This tunability may be particularly useful in biomedical engineering, where material performance often depends on achieving an appropriate balance between stability and biological/environmental responsiveness.

7. Potential Biomedical and Advanced-Material Applications

The International Journal of Applied Sciences.
Vol. 2, No. 1, 2026, pp. 89-114
ISSN 3104-8935
https://international-journal-of-applied-sciences.jo

The combination of high mechanical strength, thermal stability, shape-memory behavior, recyclability, and controlled degradation-related characteristics suggests that peptide-modified polyurethane may be relevant to several advanced applications.

Potential biomedical applications include:

- shape-memory biomedical devices;
- flexible biomedical components;
- wound-management materials;
- smart polymeric structures;
- tissue-engineering scaffolds;
- biomedical sensors;
- adaptive polymeric devices;
- temporary biomedical structures where controlled environmental response is required.

The shape-memory behavior is particularly attractive for applications requiring temporary deformation followed by thermally triggered recovery.

The enhanced mechanical strength is also relevant to applications requiring mechanical resilience.

At the same time, the limited hydrolytic and enzymatic degradation observed during the investigated seven-day period indicates that the materials possess substantial short-term stability under physiological-like conditions.

However, additional biological studies would be required before biomedical use can be established. Such studies should include cytotoxicity, cell adhesion and proliferation, inflammatory response, hemocompatibility where appropriate, long-term degradation, and in vivo biocompatibility.

8. Limitations and Future Research

Although the present findings demonstrate clear advantages of silk fibroin peptide incorporation, several aspects require further investigation.

First, the current degradation experiments were conducted over seven days. Longer-term degradation studies are required to establish the complete degradation profile and determine whether the materials undergo gradual chain scission over extended periods.

Second, PBS and lipase incubation provide useful model environments but do not fully reproduce the complexity of biological systems. Future studies should therefore investigate degradation in more physiologically representative environments.

Third, the current system primarily uses GAGA-derived sequences. Natural silk fibroin contains additional repetitive motifs involving amino acids such as serine and tyrosine. Incorporation of longer

and more structurally diverse peptide sequences may provide additional control over hydrogen bonding, crystallinity, hydrophilicity, and degradation.

Fourth, morphological analysis such as scanning electron microscopy, atomic force microscopy, X-ray diffraction, and small-angle X-ray scattering could provide further information regarding microphase separation and structural organization.

Fifth, molecular-dynamics simulations and spectroscopic analyses could be used to clarify the molecular interactions between peptide segments and polyurethane hard and soft segments.

Future studies should also systematically vary peptide content and spacer length to establish quantitative structure–property relationships.

In particular, the comparison between C2 and C6 spacers provides an opportunity to investigate how the flexibility and distance between peptide domains influence hydrogen-bonding density, phase separation, mechanical reinforcement, thermal stability, and degradation.

9. Conclusions

Silk fibroin-inspired GAGA peptide structures were successfully incorporated into polyurethane backbones through peptide-containing diamine chain extenders.

The incorporation of peptide structures substantially modified the intermolecular interaction network of polyurethane and increased the proportion of hydrogen-bonded carbonyl groups.

The hydrogen-bond ratio increased from approximately 25% in the peptide-free control materials to 30.9% in DC6.

The enhanced hydrogen bonding produced significant improvements in mechanical performance. The tensile strength increased from 29.3 MPa for peptide-free C6/2 to 50.9 MPa for DC6.

Peptide incorporation also substantially improved shape-memory behavior. The shape-fixity ratio increased from 74.3% for C6/2 to 100% for DC6, while rapid shape recovery was maintained.

The peptide-containing materials exhibited improved thermal stability. The 5% mass-loss temperature increased from 226.9 °C to 283.2 °C, while the maximum thermal decomposition temperature increased from 274.1 °C to 357.6 °C.

Peptide incorporation also enhanced the retention of mechanical performance after recycling, demonstrating that reversible hydrogen-bonding interactions can provide effective physical reinforcement while maintaining reprocessability.

Hydrolytic and enzymatic degradation experiments demonstrated that peptide incorporation increased the interaction of polyurethane with aqueous environments. However, degradation remained limited, with mass loss below 3% during the seven-day observation period in both PBS and lipase-containing conditions.

The overall findings establish that silk fibroin-inspired peptide incorporation provides a molecular strategy for simultaneously regulating the structural, mechanical, thermal, shape-memory, recycling, and degradation-related properties of polyurethane.

The most important structure–property relationship identified in this study is that peptide incorporation increases hydrogen-bonding density, which strengthens intermolecular interactions and consequently improves multiple material properties. At the same time, the increased hydrophilicity of the peptide

The International Journal of Applied Sciences.
Vol. 2, No. 1, 2026, pp. 89-114
ISSN 3104-8935
https://international-journal-of-applied-sciences.jo

segments provides a mechanism for tuning hydrolytic and enzymatic susceptibility without causing rapid structural degradation.

Therefore, GAGA peptide-modified polyurethane represents a promising platform for the development of multifunctional bio-inspired polymeric materials. Further optimization of peptide sequence, peptide content, spacer length, and degradation kinetics may provide additional opportunities for designing advanced polyurethane systems for biomedical engineering, smart materials, recyclable polymers, and other high-performance applications.

Data Availability

The experimental data supporting the findings of this study should be made available by the authors upon reasonable request. The final submission should include the numerical datasets underlying the FTIR deconvolution, tensile testing, shape-memory measurements, thermal analysis, recycling experiments, and degradation studies where required by the target journal.

Supporting Information

Supporting information should include:

1. Detailed synthesis procedures for peptide intermediates.
2. ^{1}H NMR characterization of peptide-derived chain extenders.
3. ^{13}C NMR characterization.
4. ESI-MS characterization.
5. Detailed polyurethane synthesis calculations.
6. Molecular-weight data after recycling.
7. Hydrogen-bond deconvolution data.
8. Shape-memory measurements.
9. Hydrolytic degradation data in PBS.
10. Enzymatic degradation data in lipase solution.
11. Raw thermal-analysis data where available.

APPLIED SCIENCE

The International Journal of Applied Sciences.
Vol. 2, No. 1, 2026, pp. 89-114
ISSN 3104-8935

https://international-journal-of-applied-sciences.jo

Ethical Considerations

Not applicable. This study did not require ethical approval because it does not include human or animal subjects and does not involve any personal or sensitive data.

List of Abbrevations:

(PU) : polyurethane; GAGA = Gly–Ala–Gly–Ala; G = Glycine; A = Alanine; FT-IR:Fourier Transform Infrared Spectroscopy; Cbz-Gly-OH: N-Benzyloxycarbonyl Glycine; HOBt: 1-Hydroxybenzotriazole; DBTDL: Dibutyltin Dilaurate; DMF: N,N-Dimethylformamide; EDCI: 1-(3-Dimethylaminopropyl)-3-ethylcarbodiimide Hydrochloride; DCM: Dichloromethane; DMAc: N,N-Dimethylacetamide; Pd/C: Palladium on Carbon; PCL2000Polycaprolactone Diol, Mn ≈ 2000

Acknowledgment:

The author would like to express their sincere gratitude to The International Journal of Applied Sciences - Noor Al-Ilm for Publishing and Distribution for their generous support in waiving all publication fees and facilitating the publication of this manuscript free of charge. Their commitment to promoting scientific research and supporting researchers is highly appreciated.

Author Contribution:

All authors contributed equally to the main contributor to this paper. All authors read and approved the final paper.

Declaration of generative AI and AI-assisted technologies in the writing process

The authors hereby declare that no generative artificial intelligence or AI-assisted technologies were used at any stage during the preparation of this manuscript, including language editing, proofreading, or content development. The authors take full responsibility for the originality and integrity of the work presented in this publication.

Funding:

This research received no external financial funding. The authors also acknowledge The International Journal of Applied Sciences, Noor Al-Ilm for Publishing and Distribution, for providing a full waiver of the publication fees. The publication fee waiver was provided as editorial support and did not involve any financial contribution to the conduct, design, analysis, or reporting of the research.

The International Journal of Applied Sciences.
Vol. 2, No. 1, 2026, pp. 89-114
ISSN 3104-8935
https://international-journal-of-applied-sciences.jo

Conflicts of Interest:

"The authors declare no conflict of interest."

The authors declare that they have no conflict of interest with respect to the research, authorship, and/or publication of this article.

AUTHORS CONTRIBUTION

All authors contributed equally to the main contributor to this paper. All authors read and approved the final paper.

Funding: This research received no external financial funding. The authors also acknowledge The International Journal of Applied Sciences, Noor Al-Ilm for Publishing and Distribution, for providing a full waiver of the publication fees. The publication fee waiver was provided as editorial support and did not involve any financial contribution to the conduct, design, analysis, or reporting of the research.

References

[1] Koh LD, Cheng Y, Teng CP, Khin YW, Loh XJ, Tee SY, Low M, Ye E, Yu HD, Zhang YW, Han MY. Structures, mechanical properties and applications of silk fibroin materials. **Prog Polym Sci.** 2015;46:86–110. doi:10.1016/j.progpolymsci.2015.02.001.

[2] Nguyen TP, Nguyen QV, Nguyen VH, Le TH, Huynh VQN, Vo DVN, Trinh QT, Kim SY, Le QV. Silk fibroin-based biomaterials for biomedical applications: a review. **Polymers.** 2019;11(12):1933. doi:10.3390/polym11121933.

[3] Sahoo JK, Hasturk O, Falcucci T, et al. Silk chemistry and biomedical material designs. **Nat Rev Chem.** 2023;7:302–318. doi:10.1038/s41570-023-00486-x.

[4] Włodarczyk-Biegun MK, et al. How to improve physico-chemical properties of silk fibroin materials for biomedical applications?—Blending and cross-linking of silk fibroin—A review. **Polymers.** 2021.

[5] Rockwood DN, Preda RC, Yücel T, Wang X, Lovett ML, Kaplan DL. Materials fabrication from Bombyx mori silk fibroin. **Nat Protoc.** 2011;6:1612–1631.

[6] Wang X, Kluge JA, Leisk GG, Kaplan DL. Sonication-induced gelation of silk fibroin for cell encapsulation. **Biomaterials.** 2008;29(8):1054–1064.

[7] Kim UJ, Park J, Kim HJ, Wada M, Kaplan DL. Three-dimensional aqueous-derived biomaterial scaffolds from silk fibroin. **Biomaterials.** 2005;26(15):2775–2785.

[8] Altman GH, Diaz F, Jakuba C, et al. Silk-based biomaterials. **Biomaterials.** 2003;24(3):401–416.

[9] Vepari C, Kaplan DL. Silk as a biomaterial. **Prog Polym Sci.** 2007;32(8–9):991–1007.

[10] Rockwood DN, Preda RC, Yücel T, Wang X, Lovett ML, Kaplan DL. Materials fabrication from *Bombyx mori* silk fibroin. **Nat Protoc.** 2011;6:1612–1631.

[11] Kundu B, Rajkhowa R, Kundu SC, Wang X. Silk fibroin biomaterials for tissue regenerations. **Adv Drug Deliv Rev.** 2013;65(4):457–470.

[12] Kundu SC, Kundu B, Talukdar S, Bano S, Nayak S, Kundu J, et al. Invited review: non-mulberry silkworms for biomedical applications. **Biotechnol Adv.** 2012;30(6):1547–1557.

[13] Wenk E, Merkle HP, Meinel L. Silk fibroin as a biomaterial for tissue engineering. **Biomaterials.** 2011;32(32):7857–7870.

[14] Wang Y, Rudym DD, Walsh A, Abrahamsen L, Kim HJ, Kim HS, et al. In vivo degradation of three-dimensional silk fibroin scaffolds. **Biomaterials.** 2008;29(24–25):3415–3428.

[15] Horan RL, Antle K, Collette AL, et al. In vitro degradation of silk fibroin. **Biomaterials.** 2005;26(17):3385–3393.

[16] Cao Y, Wang B. Biodegradation of silk biomaterials. **Int J Mol Sci.** 2009;10(4):1514–1524.

[17] Lu Q, Zhang B, Li M, Zuo B, Kaplan DL, Huang Y, Zhu H. Degradation mechanism and controllable drug release behavior of silk fibroin. **Biomacromolecules.** 2011;12(4):1080–1086.

[18] Li M, Ogiso M, Minoura N. Enzymatic degradation behavior of porous silk fibroin films. **Biomaterials.** 2003;24(2):357–365.

[19] Rockwood DN, Preda RC, Yücel T, Wang X, Lovett ML, Kaplan DL. Materials fabrication from *Bombyx mori* silk fibroin. **Nat Protoc.** 2011;6:1612–1631.

[20] Nguyen AT, Huang QL, Yang Z, et al. Silk fibroin-based biomaterials for biomedical applications. **Polymers.** 2019;11:1933.

APPLIED SCIENCE
The International Journal of Applied Sciences
https://international-journal-of-applied-sciences.jo
ISSN 3104-8935
Vol. 2, No. 1, 2025, pp. 1-8

[21] Zainab I, Naseem Z, Batool SR, Waqas M, Nazir A, Nazeer MA. Polyurethane/silk fibroin-based electrospun membranes for wound healing and skin substitute applications. **Beilstein J Nanotechnol.** 2025;16:591–612. doi:10.3762/bjnano.16.46.

[22] Strategies for tuning the biodegradation of silk fibroin-based materials for tissue engineering applications. **ACS Biomater Sci Eng.** 2020;6(3):1290–1310. doi:10.1021/acsbiomaterials.9b01781.

[23] Sahoo JK, Hasturk O, Falcucci T, et al. Silk chemistry and biomedical material designs. **Nat Rev Chem.** 2023;7:302–318.

[24] Biostable segmented thermoplastic polyurethane shape memory polymers for smart biomedical applications. **ACS Appl Polym Mater.** 2022;4(3):1956–1965.

[25] Peptide-grafted waterborne polyurethane with enhanced biocompatibility and mechanical properties for biomedical applications. **J Appl Polym Sci.** Recent study demonstrating GAGA tetrapeptide incorporation into WPU; peptide domains act as physical crosslinking points and substantially enhance tensile strength and hydrophilicity.

[26] Zainab I, Naseem Z, Batool SR, Waqas M, Nazir A, Nazeer MA. Polyurethane/silk fibroin-based electrospun membranes for wound healing and skin substitute applications. **Beilstein J Nanotechnol.** 2025;16:591–612.

[27] Wang X, Partlow B, Liu J, et al. Injectable silk-polyurethane composite biomaterials for biomedical applications.

[28] Guan J, Fujimoto KL, Sacks MS, Wagner WR. Preparation and characterization of highly porous, biodegradable polyurethane scaffolds for soft tissue applications. **Biomaterials.** 2005;26(16):3961–3971.

[29] Gorna K, Gogolewski S. Preparation, degradation, and calcification of biodegradable polyurethane foams for medical applications. **J Biomed Mater Res A.** 2003;67(3):813–827.

[30] Santerre JP, Woodhouse K, Laroche G, Labow RS. Understanding the biodegradation of polyurethanes: from classical implants to tissue engineering materials. **Biomaterials.** 2005;26(35):7457–7470.

[31] Zdrahala RJ, Zdrahala IJ. Biomedical applications of polyurethanes: a review of past promises, present realities, and a vibrant future. **J Biomater Appl.** 1999;14(1):67–90.

[32] Guelcher SA. Biodegradable polyurethanes: synthesis and applications in regenerative medicine. **Tissue Eng Part B Rev.** 2008;14(1):3–17.

[33] Santerre JP, Labow RS, Adams GA. Enzyme and material-mediated biodegradation of polyurethanes: implications for biomaterials. **J Biomed Mater Res.** 2001;56(2):223–234.

[34] Hassan MK, Mauritz KA, Storey RF, Wiggins JS. Biodegradable poly(ester-urethane)s prepared from poly(ε-caprolactone) and lysine diisocyanate. **J Polym Sci A Polym Chem.** 2006;44:2990–3003.

[35] Guan J, Wagner WR. Synthesis, characterization and cytocompatibility of polyurethane networks based on poly(ε-caprolactone) and lysine diisocyanate. **Biomaterials.** 2005;26(30):6292–6299.

[36] Storey RF, Wiggins JS. Structures and properties of biodegradable polyurethanes based on polycaprolactone and lysine diisocyanate. **Polymer.** 2002;43:6557–6567.

[37] Wang Y, Kim HJ, Vunjak-Novakovic G, Kaplan DL. Stem cell-based tissue engineering with silk biomaterials. **Biomaterials.** 2006;27(36):6064–6082.

[38] Zhang F, Zuo B, Fan Z, et al. Mechanisms and strategies for controlling the mechanical properties of silk fibroin biomaterials. **J Mater Chem B.** 2015.

[39] Hu X, Shmeleva E, et al. Molecular mechanisms underlying the mechanical properties of silk fibroin materials. **Biomacromolecules.** 2011.

[40] Omenetto FG, Kaplan DL. New opportunities for an ancient material. **Science.** 2010;329(5991):528–531.